

Rugby-ball-like Photonic Crystal Supraparticles with Non-Close-Packed Structures and Multiple Magneto-Optical Responses

Jingjing Liu, Mengqi Xiao, Chaoran Li, Hai Li, Zhiyi Wu, Qishan Zhu, Rujun Tang,
Ao Bo Xu, Le He**

Dr. J. Liu, M. Xiao, Dr. C. Li, H. Li, Z. Wu, Prof. L. He

Institute of Functional Nano & Soft Materials (FUNSOM), Jiangsu Key Laboratory for Carbon-Based Functional Materials & Devices, Soochow University, Suzhou, 215123, PR China

E-mail: lehe@suda.edu.cn; crli@suda.edu.cn

Q. Zhu, R. Tang

Jiangsu Key Laboratory of Thin Films, College of Physics, Soochow University, Suzhou, 215006, Jiangsu, PR China.

A.B. Xu

Department of Chemistry, the University of Western Ontario, London, Ontario N6A 3K7, Canada

Electronic Supplementary Information

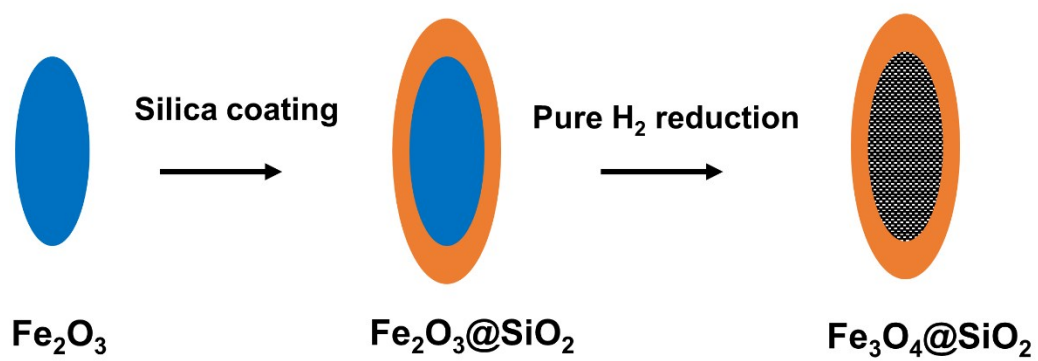


Figure S1. Schematic illustration of the preparation process of Fe₃O₄@SiO₂ nanoellipsoids.

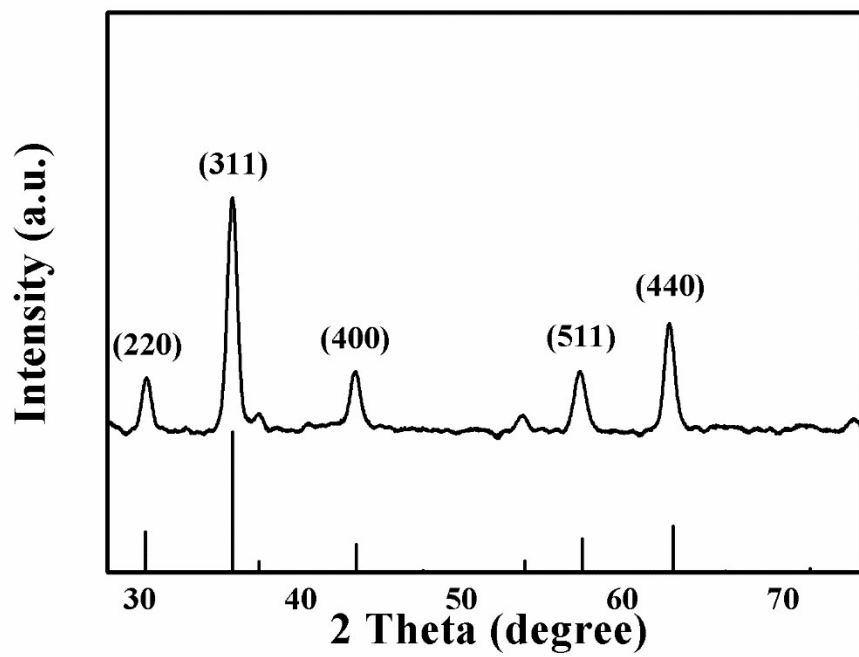


Figure S2. X-ray diffraction (XRD) pattern of the Fe₃O₄@SiO₂ nanoellipsoids.

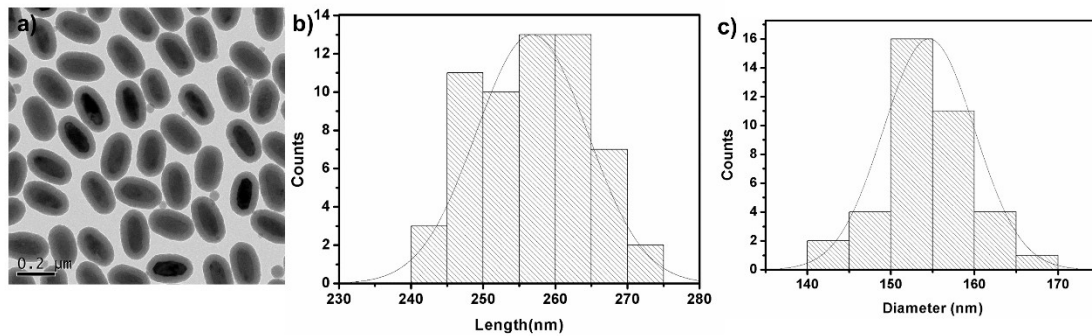


Figure S3. (a) TEM image of $\text{Fe}_3\text{O}_4@\text{SiO}_2$ nanoellipsoids. (b) Their average length, obtained by measuring 100 particles, is 250 ± 10 nm. (c) Their average diameter, obtained by measuring the same 100 particles, is 150 ± 5 nm.

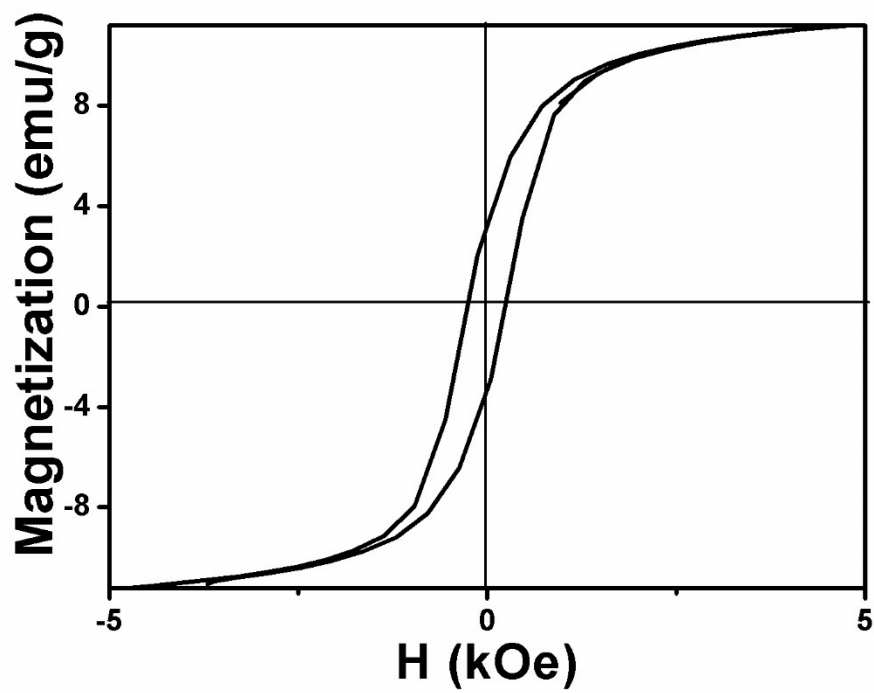


Figure S4. Hysteresis loop of $\text{Fe}_3\text{O}_4@\text{SiO}_2$ nanoellipsoids at a temperature of 300 K.

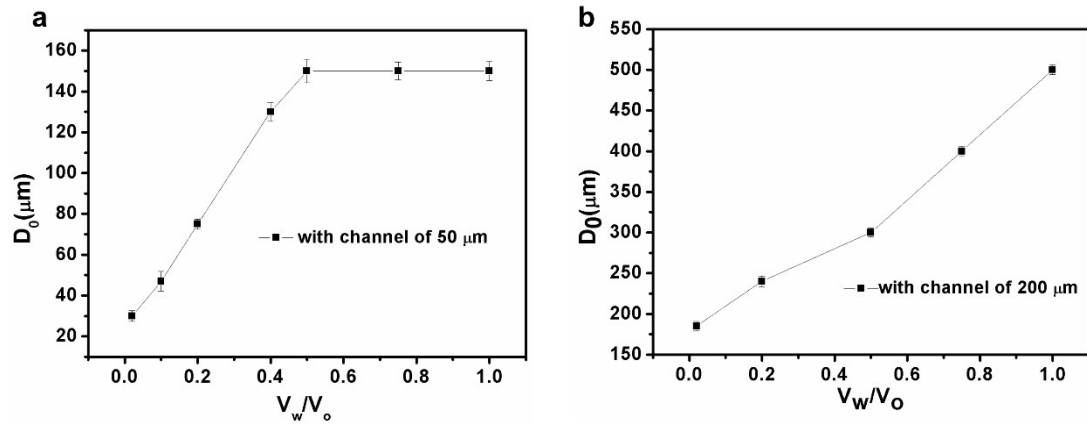


Figure S5. Relationship between the droplets size D_0 and the ratio of the velocity of water phase V_w ($\mu\text{l/s}$) to the velocity of oil phase V_o ($\mu\text{l/s}$). a. Microfluidic chip with a cross channel ($50 \mu\text{m}$ in width), b. Microfluidic chip with a cross channel ($200 \mu\text{m}$ in width)

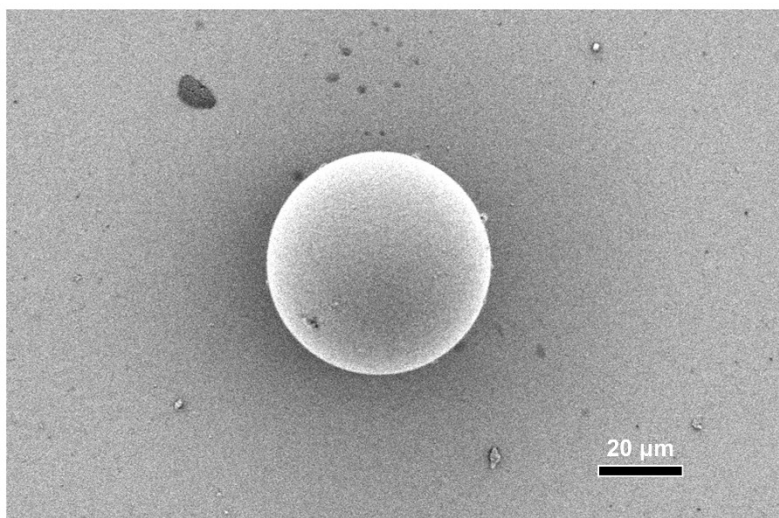


Figure S6. SEM image of a nanoellipsoids-based supraparticle dried in the absence of the external magnetic field.

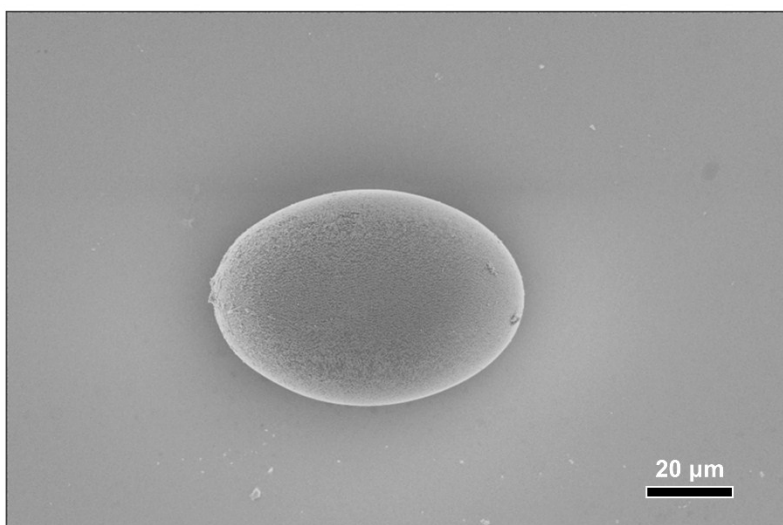


Figure S7. SEM image of a nanoellipsoids-based supraparticle dried in the presence of an external magnetic field of 95 Oe.



Figure S8. SEM image of a nanoellipsoids-based supraparticle dried in the presence of an external magnetic field of 470 Oe.

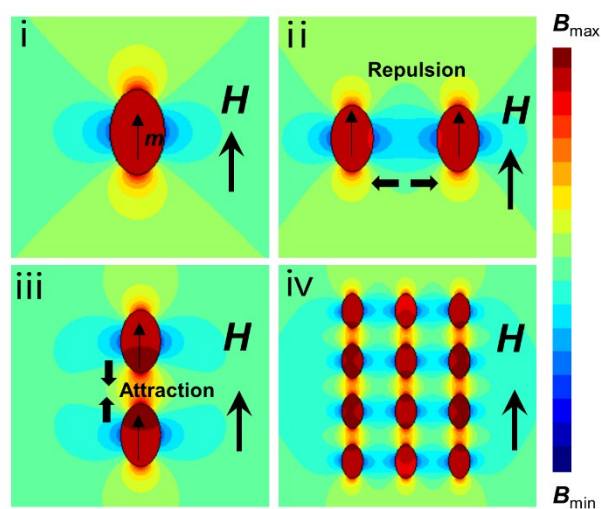


Figure S9. Simulated local magnetic field strength distributions of (i) a magnetic ellipsoid, (ii) two magnetic ellipsoids with the side-by-side configuration, (iii) two magnetic ellipsoids with the head to head configuration, and (iv) chains of magnetic ellipsoids along the external magnetic field. The directional dipolar forces between the particles (ii and iii) drives the formation of chain-like assemblies along the field direction (iv).

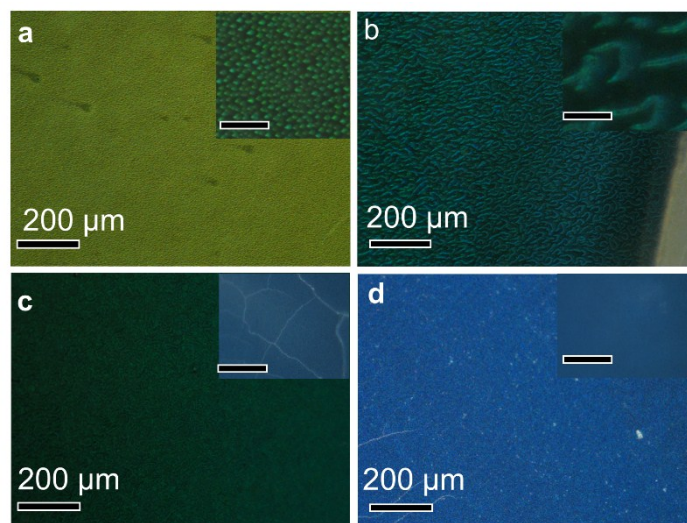


Figure S10. Optical microscope images showing the magnetic assembly of $\text{Fe}_3\text{O}_4@\text{SiO}_2$ nanoellipsoids during the drying without the spherical confinement of droplet by sandwiching the particle suspension between two glass slides. The direction of magnetic field is parallel to the viewing angle. Inserts are corresponding enlarged images with adjusted contrast to clearly show the assembled patterns. The scale bars are $20\ \mu\text{m}$ for inserts.

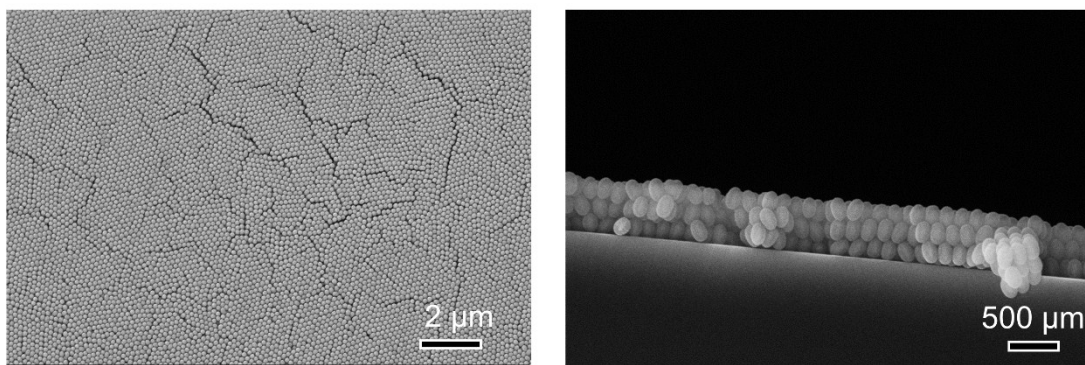


Figure S11. SEM images of the dried film of Fe₃O₄@SiO₂ nanoellipsoids without the spherical confinement of droplet.

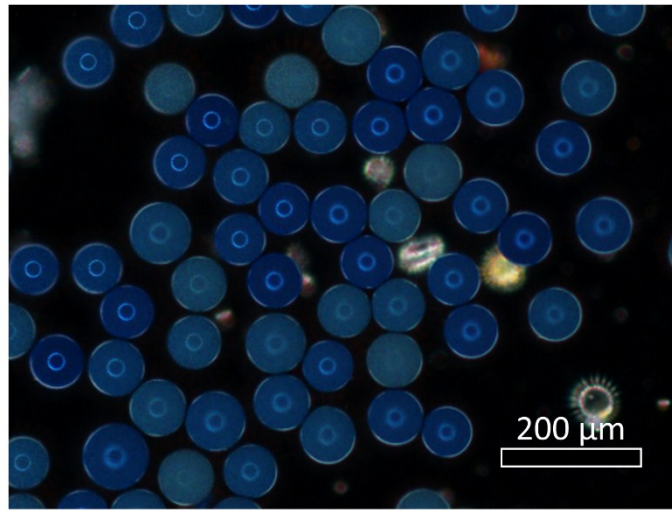


Figure S12. Dark-field optical microscope image of nanoellipsoids-based supraparticles dried in the absence of the external magnetic field.

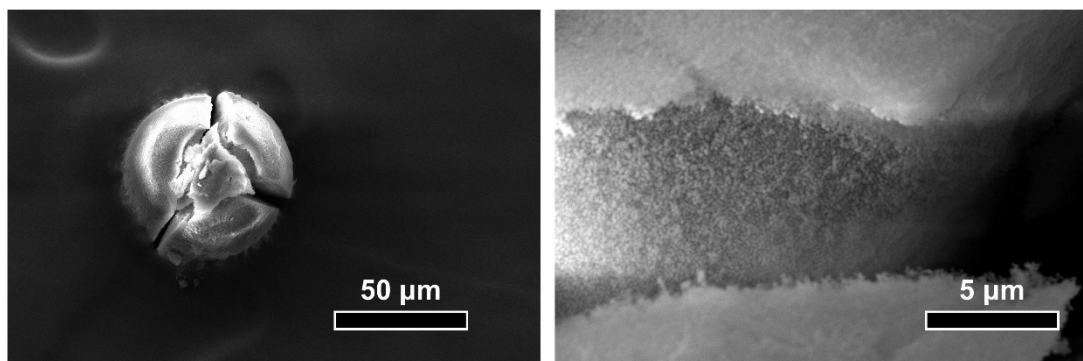


Figure S13 SEM images of a nanoellipsoids-based supraparticle dried in the absence of the external magnetic field spherical PCSs.

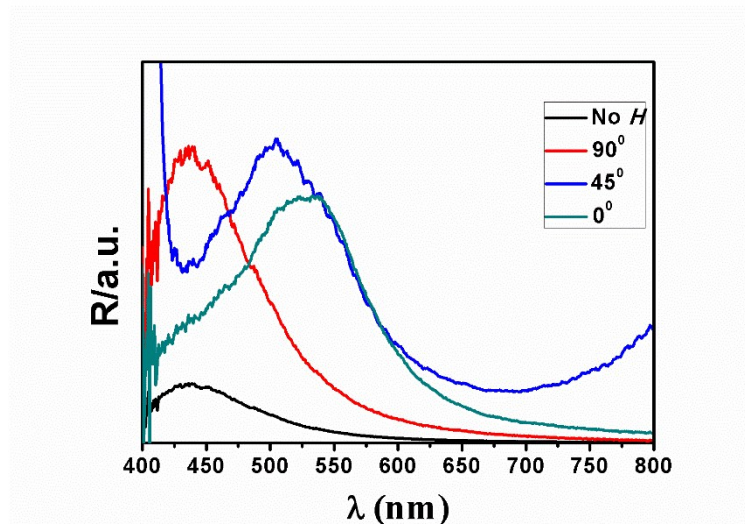


Figure S14. Reflection spectra of nanoellipsoids-based PCSs (for samples shown in Figure 5 of the main text) under magnetic fields with varying directions with respect to the direction of light.

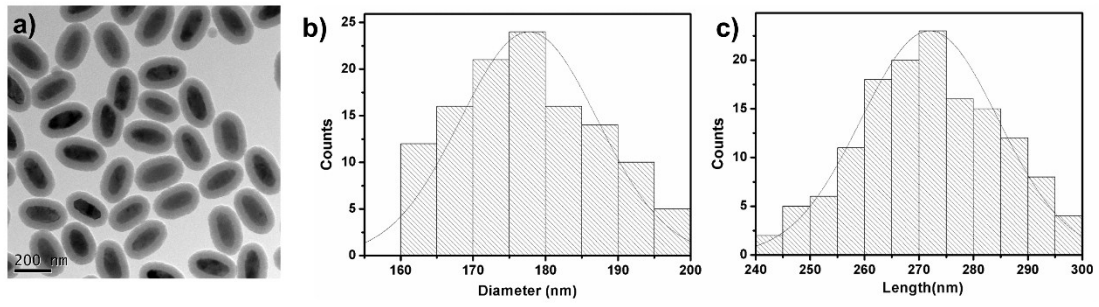


Figure S15 (a) TEM image of $\text{Fe}_3\text{O}_4@\text{SiO}_2$ nanoellipsoids. (b) Their average length is 270 ± 10 nm. (c) Their average diameter is 180 ± 5 nm.

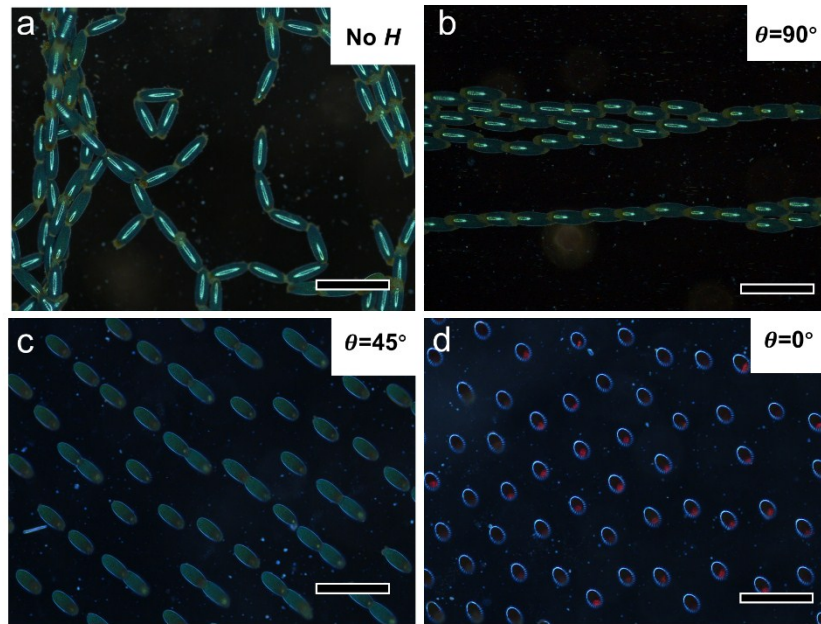


Figure S16 Dark-field optical microscope images showing magnetic tuning of structural color of PCSs made from 270 nm \times 180 nm nanoellipsoids.

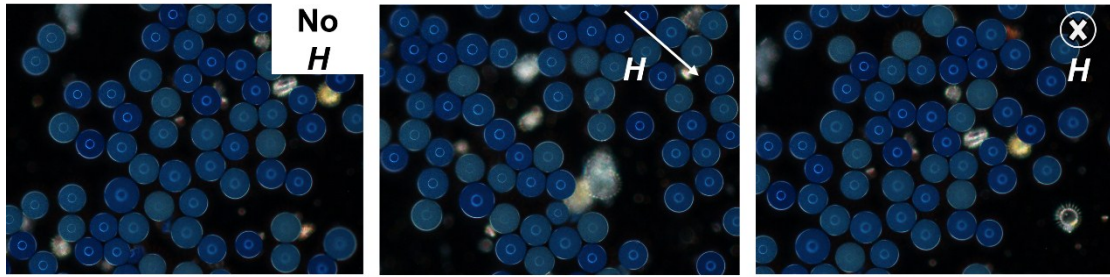


Figure S17. Dark-field optical microscope images of nanoellipsoids-based supraparticles dried in the absence of the external magnetic field spherical PCSs. These supraparticles do not show similar optical responses to magnetic fields.

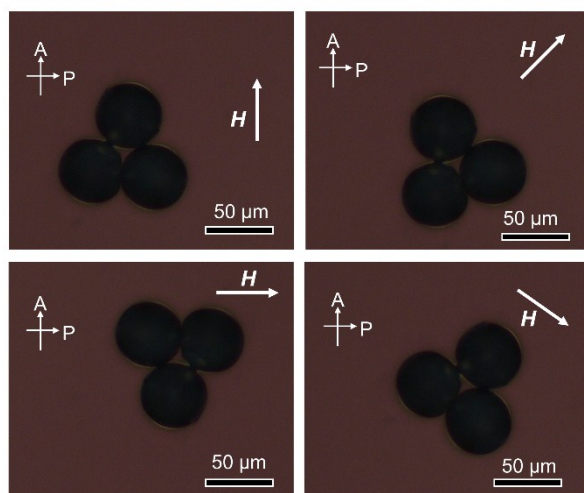


Figure S18. POM images of nanoellipsoids-based supraparticles dried in the absence of the external magnetic field spherical PCSs. These supraparticles do not show similar optical responses to magnetic fields.

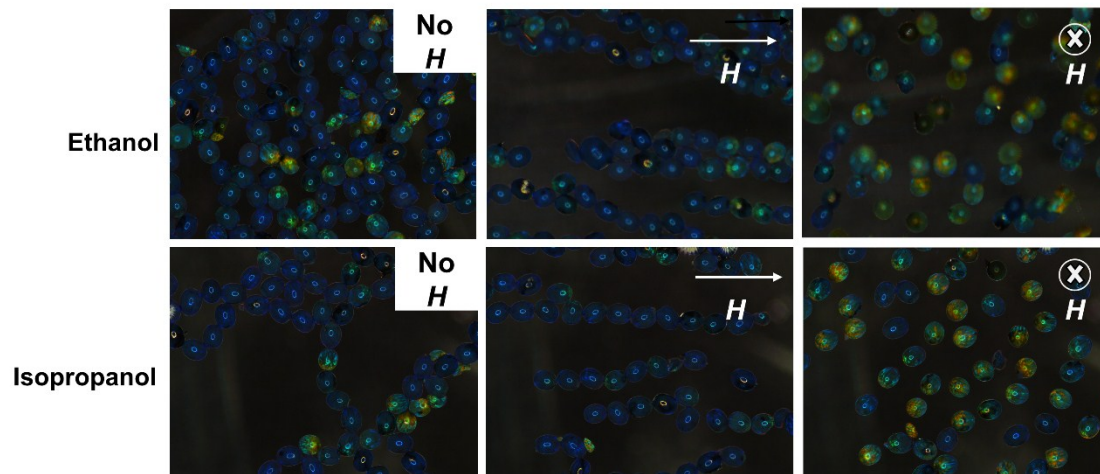


Figure S19. Dark-field optical microscope images showing the magneto-optical responses of nanoellipsoids-based PCSs (the same sample shown in Figure 5 of the main text) dispersed in ethanol and isopropanol.

Supplementary Videos

Video S1 Magnetic tuning of structural color of the Free-standing PCSs by changing the angle between the magnetic field and the incident light.

Video S2 Magnetic tuning of optical switching of free-standing PCSs by changing the angle between the magnetic field and the polarizer